2008 IEEE International Conference on
Robotics and Automation
Pasadena, CA, USA, May 19-23, 2008

Transportation of Hard Disk Media using Electrostatic Levitation and Tilt Control

Ewoud van West, Akio Yamamoto, *Member, IEEE*, and Toshiro Higuchi, *Member, IEEE*

***Abstract*— In electrostatic levitation systems, thin flat objects, such as silicon wafers, can be levitated by controlling the electric field between object and an electrode pattern, depending on the measured gap between them. This allows to manipulate these objects without making physical contact. As the gap between object and electrodes is actively controlled, the system is fairly robust for accelerations perpendicular to the objects surface. However, the restoring force for any lateral disturbance is much lower, as it is not actively controlled. This restricts the allowable lateral accelerations and poses a serious limitation on practical implementation of electrostatic levitation system as a good non-contact object handler. In this paper, the allowable lateral accelerations are increased by tilting the electrodes and object during lateral acceleration. Experimental results show how with tilting control, a levitated aluminium disk always remains aligned with the electrodes, while without tilt control it oscillates around the central point.**

I. INTRODUCTION

In electrostatic levitation, an object is levitated by controlling an attractive electrostatic force on it. The attractive force is generated by an electric field that exists between an electrode pattern (the levitator) and the object, when a high voltage is applied to the electrodes. Although the principle is analogous to magnetic levitation, there are some distinct properties that exceed some limitations that are present in magnetic levitation, the most important one being able to levitate a great variety of materials including conductors [1], semiconductors such as silicon wafers [2], and even dielectrics like glass [3]. However, the electrostatic force is relatively weak compared to magnetic levitation systems of the same size, and this requires high voltage levels, small air gaps, and relatively large areas, to create an attractive force that is strong enough to compensate the gravitational force. However, for objects such as silicon wafers, for which the thickness is many times smaller as the diameter, electrostatic levitation can be a very suitable replacement for a conventional contact-based spatula. The most prominent advantages are: no contamination, because physical contact is avoided, and no structural deformation as the attractive force is distributed over the total area. Possible applications include non-contact handling of silicon wafers or thin glass plates (e.g. from flat panel displays), which can be either fully automated, or human operated [4].

This work was partly supported by a Grant-in-Aid for Scientific Research, No. 18360117, from MEXT in Japan.

E. van West, A. Yamamoto, and T. Higuchi are with the Advanced Mechatronics Lab, Department of Precision Engineering, School of Engineering, the University of Tokyo, 7-3-1, Hongo, Bunkyo-ku, Tokyo 113-8656, Japan {ewoud, akio, higuchi}@aml.t.u-tokyo.ac.jp

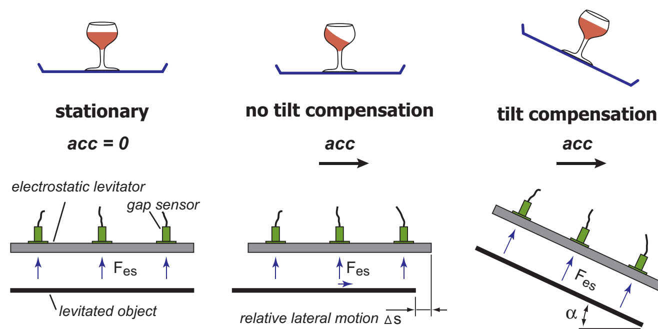

Fig. 1. Tilt control allows for larger lateral accelerations as relative motion of disk Δs with respect to levitator remains zero

In electrostatic levitation systems, the attractive suspension force is actively controlled, which gives the levitated object positive stiffness around a preset air gap. There is also a passive lateral restoring force that will keep the object aligned with the electrodes due to the edge effect [5]. For electrostatic levitation systems levitating conductors and semi-conductors, this lateral stiffness is much lower than the suspension system (order 4), giving limitations on the allowable lateral disturbances. These limitations can give problems in object handling systems or even in a MEMS force balance electrostatic accelerometer [6]. In case of electrostatic levitation systems levitating dielectrics, such as glass, the lateral restoring stiffness is higher (roughly 20 times bigger [3]), making it more robust in comparison with levitation systems for conductors and semi-conductors.

To make a practical non-contact handling system for conductors and semi-conductors, levitation alone is not sufficient. The loading, releasing, and especially the transporting of the object are crucial tasks that also have to be considered. Loading and releasing has already been successfully realized in previous research [7]. For transporting, a system has been developed that integrates levitation and transportation of the object in one system (Direct Electrostatic Levitation and Propulsion system, DELP [8]). It uses the lateral force to move the levitated object by activating a different set of electrodes, which have a pitch with respect to the previously active electrodes. As the lateral force is very weak, the maximum acceleration and speed that can be realized for conductors and semi-conductors is low (order 10 mm/s). Another disadvantage of this system is that if if the transportation path increases, the required number of gap sensors increases proportionally, which can become costly. Another solution is to attach the levitation system at the end-effector

of a manipulator. In this case, the maximum acceleration with which the manipulator can move the levitation system in a lateral motion, is limited by the weak lateral restoring force. The levitated object can not follow high accelerations of the levitator and will resultantly drop. This poses a serious limitation on the practical implementation of such a system.

In this paper, a technique is proposed to increase the allowable lateral accelerations by tilting the electrostatic levitator during lateral accelerations. This approach, which is also illustrated in Fig. 1, is similar to the technique waiters use in restaurants to serve beverages quickly, but without spilling the content. In case of electrostatic levitation, by tilting the levitator and the object, the attractive force perpendicular to the object's surface is also used for the object to follow the acceleration of the levitator.

The concept of tilting an object during accelerations is not unique, and related research can be found in liquid transportation systems to prevent "sloshing" [9] [10]. Also, some research has been done with magnetic levitation in handling production steel plates [11]. However, applying tilt control to an electrostatic levitation and transportation system has not been reported.

The structure of this paper is as follows: in Section II, the theory of electrostatic levitation is introduced. Then Section III describes the tilt control for electrostatic levitation in more detail. Section IV shows the details of the experimental setup, while results are presented in Section V.

II. ELECTROSTATIC LEVITATION [1] [2]

This section describes very briefly the basic principle of electrostatic levitation, a technique which has been employed in a variety of fields, such as a vacuum gyro [12], microbearings [13], and object handling [14]. It is based on literature [1] [2] where more details can be found.

The principle of electrostatic levitation is schematically shown in Fig. 2(a). An attractive electrostatic force can be generated by creating an electric field between object and electrodes. The electrostatic force follows

$$f = \frac{\varepsilon_0 A V^2}{2z^2}, \tag{1}$$

where A is the active area, V the voltage applied to the electrode, ε_0 the permittivity of air, and z is the air gap and the electric field E is defined as V/z.

The intensity of the electric field can not be increased indefinitely as at a certain threshold value E_{max}, electric discharge will occur. In atmospheric conditions, a typical value of 3 kV/mm is used as the upper limit and this limits the available maximum electrostatic force intensity to approximately 4 mN/cm^2. In vacuum conditions, the maximum field intensity is much higher, and thus larger forces can be obtained.

Active control, such as position feedback, is necessary as passive electrostatic levitation is unstable (Earnshaw's theorem). The force equation (1) can be linearized around an operating point (f_e, V_e, z_e) in which for bias voltage V_e, there is an equilibrium air gap z_e where the attractive

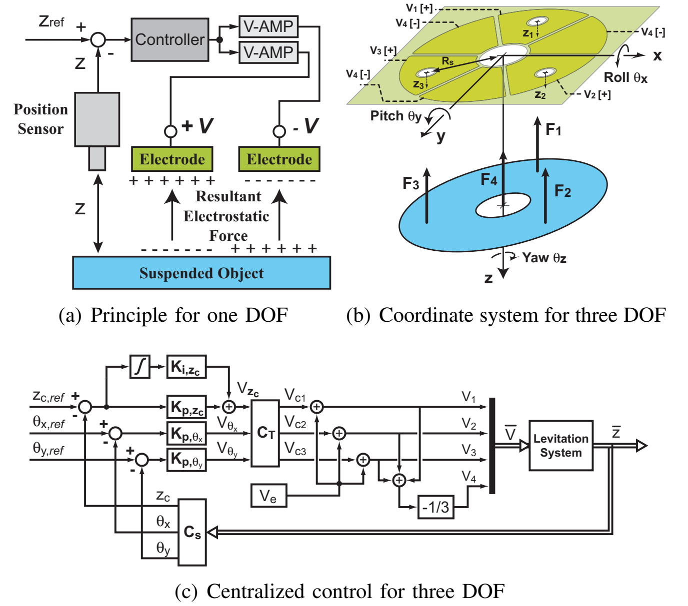

(a) Principle for one DOF

(b) Coordinate system for three DOF

(c) Centralized control for three DOF

Fig. 2. Principle for one and three DOF electrostatic levitation

electrostatic force equals the gravity force on the object $(f_e = mg)$. With deviations from the linearization point defined as

$$z = z_e + \tilde{z}, \quad \text{and} \quad V = V_e + \tilde{V}, \tag{2}$$

this results in

$$f = K_v \tilde{V} - K_z \tilde{z} + f_e, \tag{3}$$

where

$$K_v = \frac{\varepsilon_0 A V_e}{z_e^2}, \quad K_z = \frac{\varepsilon_0 A V_e^2}{z_e^3} \quad \text{and} \quad f_e = \frac{\varepsilon_0 A V_e^2}{2 z_e^2}$$

If at air gap z_e, the maximum attractive force that can be realized without electric discharge is

$$f_{max} = \frac{1}{2}\varepsilon_0 A E_{max}^2, \tag{4}$$

the force ratio between nominal and maximum force can be defined as

$$n = \frac{f_e}{f_{max}} = \left(\frac{E_e}{E_{max}}\right)^2, \tag{5}$$

which can be used in calculations for tilt control in the next section.

From (3) it is clear that by controlling the voltages applied to the electrodes, the air gap between object and electrodes can be regulated. For more DOF, such as the levitation of an aluminium disk, (3) can be extended by writing it in vector and matrix form. The disk can be levitated by controlling only 3 degrees of freedom (DOF), namely the translational vertical z-motion and the two rotational roll and pitch motions. The lateral translation motions (x, y-direction) of the disk have a passive restriction as a result of the active vertical control (z-direction) so that when the disk slips out of the central position, a restoring force will return it [5]. Calculating the theoretical value of the lateral restoring force

as a function of the lateral motion is fairly complex, not only due to the geometrical shape of disc and electrode pattern, but also because of the interaction between levitation force and lateral restoring force. A simple approximation in which levitation gap is fixed, can be determined by using only the change in capacitance and is given by [15]:

$$F_{lat} = \frac{\varepsilon_0 V_e^2}{z_e^2}\left[\sqrt{R_o^2 - \frac{s^2}{4}} + \sqrt{R_i^2 - \frac{s^2}{4}}\right], \qquad (6)$$

where R_i and R_o are the inner and outer diameter of the disk, and s is the relative lateral motion between disk and levitator

A coordinate system is defined in Fig. 2(b), where $x, y,$ and z represent the centralized coordinates and z_i, $(i = 1, 2, 3)$ are the local air gaps measured by the gap sensors. For each DOF, there is an electrode pair (positive and negative), which is distributed as shown in Fig. 2(b). However, the negative electrodes all share the same potential (V_4). Values in the centralized coordinate system can be derived from the local z_i using transformation matrix C_S:

$$\begin{bmatrix} z_c \\ \theta_x \\ \theta_y \end{bmatrix} = \underbrace{\begin{bmatrix} 1/3 & 1/3 & 1/3 \\ \frac{-2}{3R_s} & \frac{1}{3R_s} & \frac{1}{3R_s} \\ 0 & \frac{-1}{\sqrt{3}R_s} & \frac{1}{\sqrt{3}R_s} \end{bmatrix}}_{C_S} \times \begin{bmatrix} z_1 \\ z_2 \\ z_3 \end{bmatrix}, \qquad (7)$$

under the assumption that for small angles $\sin(\theta) = \theta$ and R_s is the distance from the sensor to the origin of the coordinate system.

Stable levitation is realized by active feedback control using a centralized control scheme as is shown in Fig. 2(c). The controller can consist of only proportional K_p-terms, as there is a natural damping effect present from the air; the air gap during stable levitation is significantly smaller than the diameter of the disk and that allows the air to be modeled as a squeeze film [16]. For the vertical z-translation however, there is also an integral term K_i, such that there is no steady state gap error. The control voltage output of each controller has to be combined and transformed into the correct electrode voltages using transformation matrix C_T, which is the negative transpose matrix of C_S: $C_T = -(C_S)^T$.

III. TILT CONTROL

In this section, the tilt control of the disk is discussed. An approximated numerical example based on typical values is used to show the difference in allowable lateral acceleration when there is no tilt control, and the case with tilt control on. The values of parameters used in the numerical calculations are shown in Table I.

A. Lateral restoring force

To estimate the maximum lateral restoring force for the parameters as mentioned in Table I, (6) gives this value if the lateral motion s is zero. This gives a maximum lateral restoring force of 1.3 mN, which relates to a maximum allowable lateral acceleration of 0.09 m/s^2. Even though it is a rough estimate and better analytical results can be obtained [5], the value is close to experimental results (maximum lateral force 1.0 mN / maximum acceleration 0.07 m/s^2) and thus can be used to give an indication for the order of the maximum allowable lateral acceleration.

TABLE I
TYPICAL LEVITATION PARAMETERS

Bias Voltage	V_e	1.0 kV
Nominal air gap	z_e	400 μm
Roll and pitch	$\theta_x = \theta_y$	0°
Permittivity of air	ε_0	8.854 F/m
Outer diameter disk	R_o	47.5 mm
Inner diameter disk	R_i	12.5 mm
Weight of disk	w	14.42 g
Maximum Electric field (air)	E_{max}	3 kV/mm

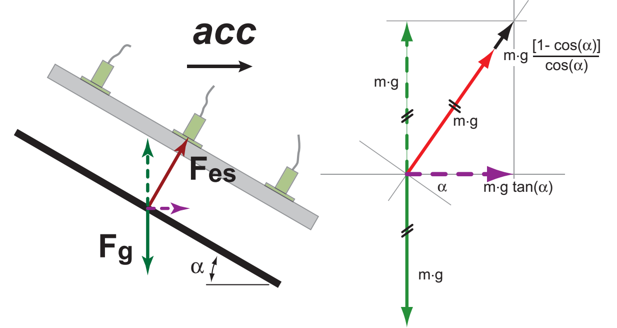

Fig. 3. Free Body Diagram of forces acting on the disk with acceleration and tilting

B. Tilting of disk

Allowable lateral accelerations can be increased by tilting of the disk, so that the attractive electrostatic force is also used during lateral translations. Basically, there would be two ways to realize a tilting angle in the disk: use the levitation controller to give a reference angle, so that only the disk itself rotates; and rotating both the levitator and the disk.

As the ratio between dimensions of the disk and levitated air gap is very large, the space to rotate the disk is very limited. Furthermore, bringing one side of the disk closer to the levitator increases the chance of touching or electric discharge. So even though this would be a simple solution, as no rotation mechanism has to be employed, the performance improvement might not be significant. This can be illustrated by a numerical example. Take the nominal gap of 400 μm and set the limit of the distance between edge of disk and levitator at 50 μm, then the maximum rotation angle would be in the order of $\alpha_{max} = \arcsin(0.35/47.5) = 0.42°$, giving a maximum allowable lateral acceleration of 0.07 m/s^2, which is in the same order as was the case of no tilt control. The final allowable maximum acceleration will be a combination of the two.

The allowable lateral accelerations can be further increased by tilting both levitator and levitated object. The strategy of tilt control will be to have a rotation mechanism tilt the

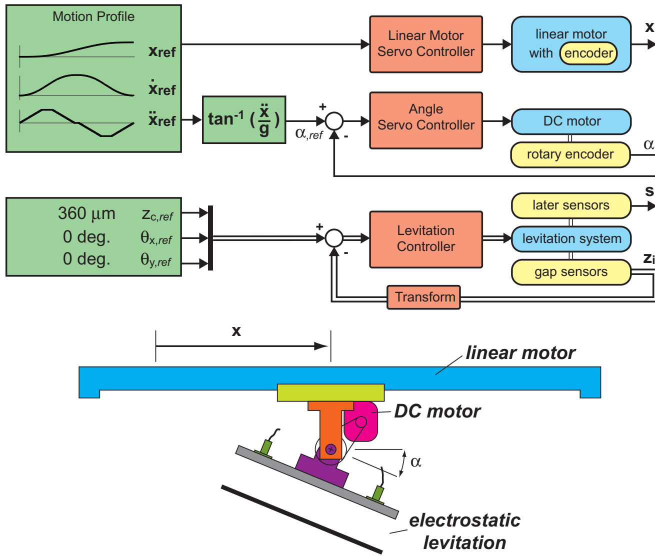

Fig. 4. Overview of experimental setup with signal flow on top and schematic drawing on the bottom

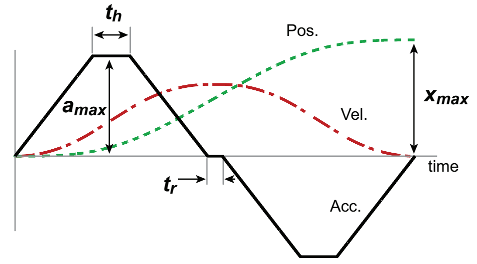

Fig. 5. Motion profile, which is determined by 4 parameters

levitator and disk by an angle α, depending on the lateral acceleration $\ddot{x}$. The angle that should be given is determined by the forces acting on the disk, namely the gravitational force F_g and the decomposed electrostatic force F_{es} that gives the inertial force for the acceleration. This is illustrated in Fig. 3 and the relationship is a simple geometric condition:

$$\cos(\alpha) = \frac{F_g}{F_{es}}, \quad (8)$$

which gives the acceleration of $\ddot{x} = g \tan \alpha$. The maximum acceleration can be found when $\cos(\alpha) = n$, which gives the following equation:

$$\ddot{x}_{max} = g \tan(\arccos(n)) = g\frac{\sqrt{1-n^2}}{n}, \quad (9)$$

A calculation example of values from Table I gives that the force ratio $n = (5/6)^2$ sets the maximum angle $\alpha_{max} = 46°$ and this gives a maximum acceleration in the order of 10 m/s^2, a result which far exceeds the other two cases. However, this simple result does not include effects such as disturbances from the surrounding air or the dynamics of the disk during rotation.

IV. EXPERIMENTAL SETUP

This section describes all components of the experimental setup, which mainly consists of three parts: a linear motor to generate controlled horizontal accelerations; an angle control mechanism to regulate the angle of levitator and disk; and the electrostatic levitation system itself. A schematic overview of the experimental setup is shown in Fig. 4. On the left side are all the reference signals that are inputs to the controllers, which control the motion of each subsystem on the right. Both reference signals and most of the controllers (the linear motor has an additional external controller) are implemented on a Digital Signal Processing (DSP) system which is running at 5 kHz. The motion profile, shown in more detail in Fig. 5, has ramp functions for the acceleration and the shape is determined by four individual parameters, namely the maximum acceleration a_{max}, the maximum or final position x_{max}, and two time parameters t_h and t_r which determine how long the maximum acceleration is kept and how much time there is between acceleration and deceleration respectively. The maximum position is limited by the stroke of the linear motor and also special concern has to be taken that the maximum velocity does not exceed the linear motor's limitation. Although the linear motor (IKO LT100CGS-200/10) has a resolution of 1μm, the step resolution is fixed at 40 μm on the DSP as a trade off between maximum speed (0.2 m/s) and accuracy.

In the electrostatic levitation setup, which is also shown in Fig. 6(a) the local air gaps z_i are measured by three eddy current sensors (Keyence EX-008, range 0 to 1 mm). Two through-beam laser sensors (Omron ZX-LT010, range 0 to 10 mm) are mounted on the side to measure the relative lateral motion of the disk with regard to the electrodes. The control parameters to realize the stable levitation are: $K_{P,z_c} = 10 \cdot 10^6$ V/m and $K_{I,z_c} = 5 \cdot 10^6$ V/(m s) for the vertical translation control, and $K_{P,\theta_x} = K_{P,\theta_y} = 0.5 \cdot 10^6$ V/rad for the rotational movements of the disk with respect to the electrodes. The reference gap is set to 360 μm and the bias voltage V_e is 1.08 kV. The controller output is connected to four high voltage D.C. amplifiers (Trek 609C-6), which have an internal gain of 1000 and are limited on the control side to 1.6 kV in absolute value to prevent electric discharge.

The rotation mechanism, shown in Fig. 6(b), to control the angle of the levitation system is realized by a DC-motor (Como Drills 719 RE450, 15Vdc) which drives a friction gear (reduction ratio 10:1) that is connected to the electrode mounting board. The friction drive mechanism reduces any play between DC-motor and the levitator. Two shafts are also connected to this mounting board with the central axis just below the electrodes, such that the center of rotation coincides with the center of the disk when it is levitated. The shafts are supported by bearings that are connected to a base plate, which also holds the DC-motor. On the other side, a laser rotary encoder (Canon K-1, 81000 pulses per rotation) is connected to the shaft through a coupling to measure the angle α. The angle is controlled by a PI-D controller with feedforward and its controller output is connected to a power amplifier (Takasago LTD., BPS120-5) to provide the driving

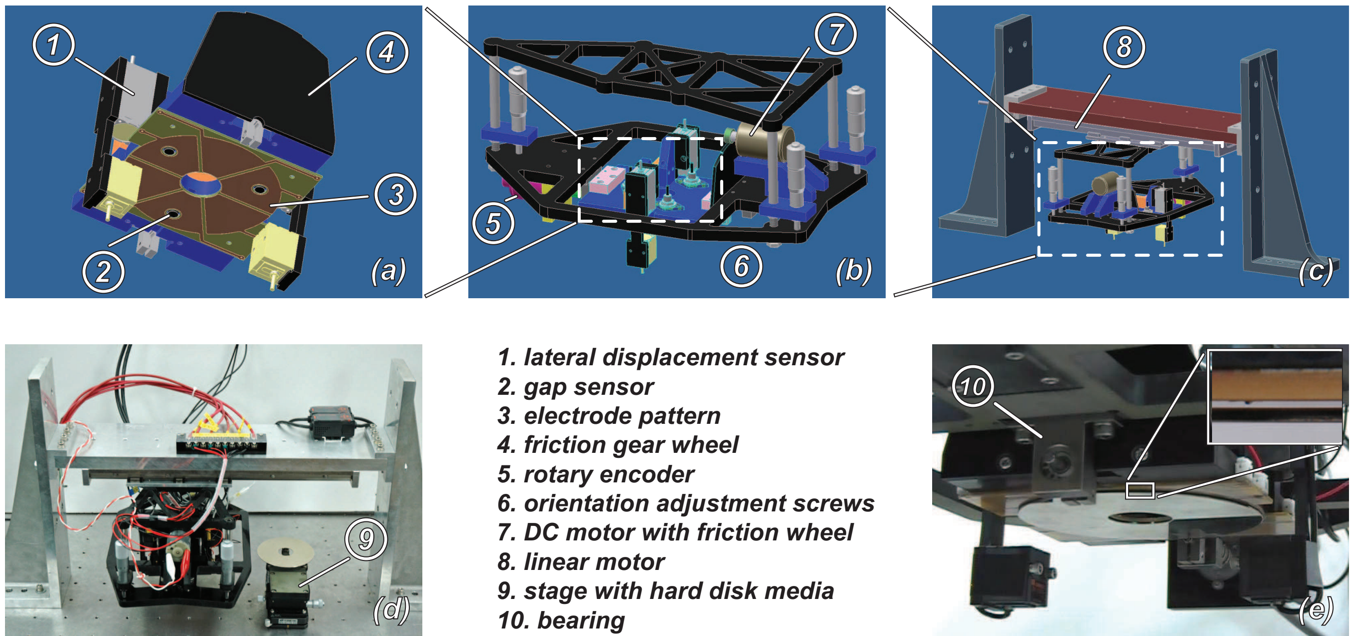

Fig. 6. Details of experimental setup. (a) electrodes with gap and lateral sensors. (b) Suspended structure with tilt control. (c) Complete structure with linear motor. (d) Photograph of setup. (e) Stable levitation of disk.

current for the DC-motor.

The base plate is connected to a upper plate by three spring preloaded shaft-micrometer combinations. This allows to adjust the orientation of the base plate through the micrometer screws to make sure it is level. The construction material for most components is bakelite as it is light and strong. The whole mechanism is connected to the linear motor that is fixed at its position by two large aluminium angles and a big aluminium block as is shown in Fig. 6(c). A photograph of the setup is given in Fig. 6(d), which also shows the aluminium disk that will be loaded by a movable z-stage. Stable levitation is shown in Fig. 6(e), where the air gap is 360 μm.

V. EXPERIMENTAL RESULTS

This section shows the experimental results, which consist of the servo behavior of both linear motor and angle rotation mechanism, as well as the behavior of the disk under lateral acceleration with tilt control ON and OFF.

In the upper graph of Fig. 7, the servo behavior of the linear motor is analyzed. A motion profile ($a_{max} = 0.05$ m/s^2, $t_h = 1.5$ s, $t_r = 0.1$ s, $x_{max} = 0.22$ m) is created of which the reference position x_{ref} should be followed by the linear motor. The reference signals are dashed, while the measured position, coming from the linear encoder that is inside of the linear motor, is presented by a solid line. The linear motor follows the reference signal very well with smooth motion and little position error (middle plot). The lower graph shows how the angle rotation mechanism follows the angle reference signal. Again, the reference signal is dashed, while the measured position, coming from the rotary encoder is presented by the solid line. The same graph also shows

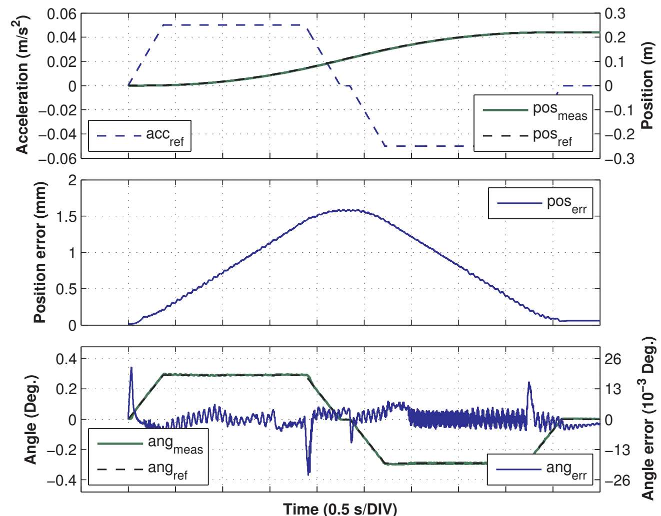

Fig. 7. Servo behavior of linear motor and tilting of levitator

the angle error. Largest errors occur where the slope of the reference angle changes.

To analyze the effect of tilt control, two situations were compared: tilt control ON; and tilt control OFF. As for high accelerations, the disk will be almost immediately lost in case of tilt control OFF, a maximum acceleration of 0.05 m/s^2 is selected, as it should be within the allowable range of lateral accelerations. Then by comparing the relative lateral motion of the disk to the electrodes during motion, conclusions can be made if the tilt control is successful. Results of the measurement are shown in Fig. 8 and as can be clearly seen in the figure when the tilt control is OFF, the relative lateral motion of the disk with respect to the levitator shows a

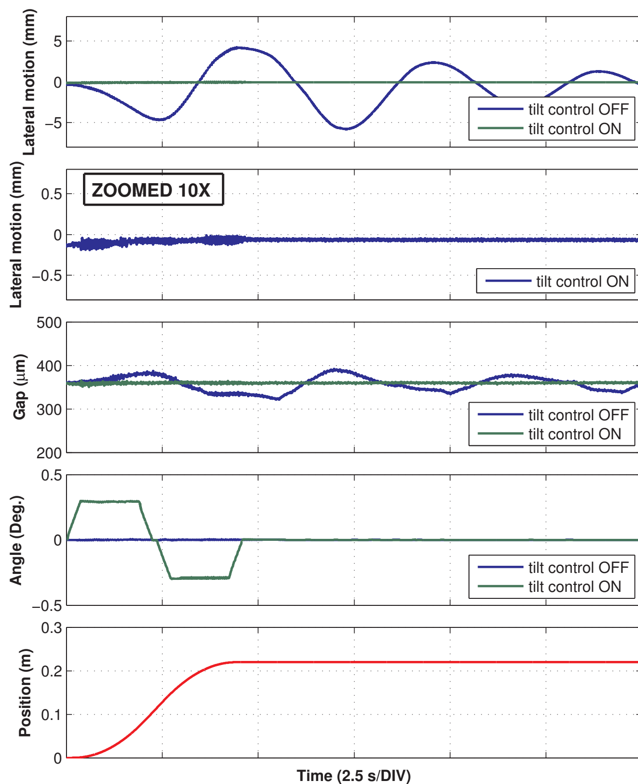

Fig. 8. Properties of levitated disk under lateral motion with tilt control ON and OFF

damped oscillating behavior of roughly 5 mm around the center, which continues even after the motion of the linear motor has ended and slowly damps out. With tilt control ON, the relative lateral motion is almost negligible compared to the results with tilt control OFF. Furthermore, no deviations of the air gap can be observed in case of tilt control ON, while when the tilt control is OFF, a maximum levitation error of 35 μm occurs, which has a direct relation with the relative lateral motion. The figure also shows the measured angle and position to indicate the start and end of the motion.

VI. CONCLUSIONS AND FUTURE WORK

The practical implications of electrostatic levitation as a non-contact handling system is restricted by a limitation in allowable lateral acceleration of the levitated object. This restriction can be compensated by tilting the object during lateral accelerations as now the attractive electrostatic force can be decomposed to balance not only the gravitational, but also the inertial forces. Limitations in this concept will come from the maximum electrostatic force that can be generated without electric discharge (maximum electric field). However, a calculation example on an aluminium disk, levitating at an air gap of 400 μm by 1 kV, shows that the lateral accelerations can be increased from 0.07 m/s^2 by a factor 150. The tilting concept is verified experimentally by an experimental setup in which the angle of the levitator can be modified during lateral acceleration. With a maximum acceleration set to 0.05 m/s^2, the relative lateral motion of the disk with the levitator becomes almost negligible with active tilt control (0.29° angle) if it is compared to a case where tilt control is off.

Future work will include experiments with higher accelerations and also a comparison with tilting of only the disk by levitation control. Furthermore, the tilting angle is now limited to 1 degree of freedom (pitch). The system can be expanded by controlling also the other rotational angle (roll). To make the levitation plus tilting mechanism more compact and suitable to mount it as an end-effector to a robotic arm, a parallel-link mechanism can be used as a substitute for the DC-motor. Also, it will be interesting to see how the system performs for less ideal acceleration profiles.

REFERENCES

[1] J. Jin, T. Higuchi, and M. Kanemoto, "Electrostatic levitator for hard disk media," *IEEE Trans. Ind. Electron.*, vol. 42, no. 5, pp. 467 – 73, 1995.

[2] J. Jin, T. Higuchi, and M. Kanemoto, "Electrostatic silicon wafer suspension," in *Fourth International Symposium on Magnetic Bearings ISMB4*, Zurich, 1994, pp. 343 – 348.

[3] J. U. Jeon and T. Higuchi, "Electrostatic suspension of dielectrics," *IEEE Trans. Ind. Electron.*, vol. 45, no. 6, pp. 938 – 46, 1998.

[4] E. van West, A. Yamamoto, B. Burns, and T. Higuchi, "Non-contact handling of hard-disk media by human operator using electrostatic levitation and haptic device," in *Proceedings International Conference on Intelligent Robots and Systems*, Oct. 2007, p. to appear.

[5] S. J. Woo, J. U. Jeon, T. Higuchi, and J. Jin, "Electrostatic force analysis of electrostatic levitation system," in *Proceedings of the 34th SICE Annual Conference SICE '95*, Japan, 1995, pp. 1347–52.

[6] T. Nakagawa, M. Hama, and T. Furukawa, "Study of magnetic levitation technique applied to steel plate production line," *IEEE Trans. Magn.*, vol. 36, no. 5, pp. 3686 – 9, Sept. 2000.

[7] E. van West, A. Yamamoto, and T. Higuchi, "Pick and place of hard disk media using electrostatic levitation," in *Proceedings of the 2007 IEEE International Conference on Robotics and Automation ICRA'07*, April 2007, pp. 2520–2525.

[8] J. Jin and T. Higuchi, "Direct electrostatic levitation and propulsion," *IEEE Trans. Ind. Electron.*, vol. 44, no. 2, pp. 234 – 9, apr 1997.

[9] K. Yano and K. Terashima, "Robust liquid container transfer control for complete sloshing suppression," *IEEE Trans. Contr. Syst. Technol.*, vol. 9, no. 3, pp. 483 – 493, 2001.

[10] S. J. Chen, B. Hein, and H. Wörn, "Using acceleration compensation to reduce liquid surface oscillation during a high speed transfer," in *Proceedings of IEEE International Conference on Robotics and Automation*, Apr. 2007, pp. 2951–56.

[11] R. Houlihan and M. Kraft, "Modelling of an accelerometer based on a levitated proof mass," *Journal of Micromechanics and Microengineering*, vol. 12, no. 4, pp. 495 – 503, 2002.

[12] H. W. Knoebel, "The electric vacuum gyro," *Control Engineering*, vol. 11, pp. 70–73, feb 1964.

[13] S. Kumar, D. Cho, and W. Carr, "Experimental study of electric suspension for microbearings," *Journal of Microelectromechanical Systems*, vol. 1, no. 1, pp. 23–30, mar 1992.

[14] E. van West, A. Yamamoto, and T. Higuchi, "Development of "haptic tweezer", a non-contact object handling system," in *Proceedings of the EuroHaptics International Conference*, Paris, 2006, pp. 87–92.

[15] J. U. Jeon, "Electrostatic suspension and its applications," Ph.D. dissertation, The University of Tokyo, March 1997.

[16] W. Griffin, H. Richardson, and S. Yamanami, "A study of fluid squeeze film damping," *ASME J. Basic Eng.*, pp. 451–56, 1966.